Supporting Information for:

Differential timing of a conserved transcriptional network underlies divergent cortical projection routes across mammalian evolution

Annalisa Paolino[a,1], Laura R. Fenlon[a,1,2], Peter Kozulin[a], Elizabeth Haines[a], Jonathan W.C. Lim[a], Linda J. Richards[a,b,2,3], and Rodrigo Suárez[a,2,3]

[a]Queensland Brain Institute, The University of Queensland, Brisbane, QLD 4072, Australia.
[b]School of Biomedical Sciences, The University of Queensland, Brisbane, QLD 4072, Australia.

[2]To whom correspondence may be addressed. Email: l.fenlon@uq.edu.au, richards@uq.edu.au, r.suarez@uq.edu.au.
[1]A.P. and L.R.F. contributed equally to this work.
[3]L.J.R. and R.S. contributed equally to this work.

This PDF includes:

www.pnas.org/cgi/doi/10.1073/pnas.1922422117

Supporting Figures

A

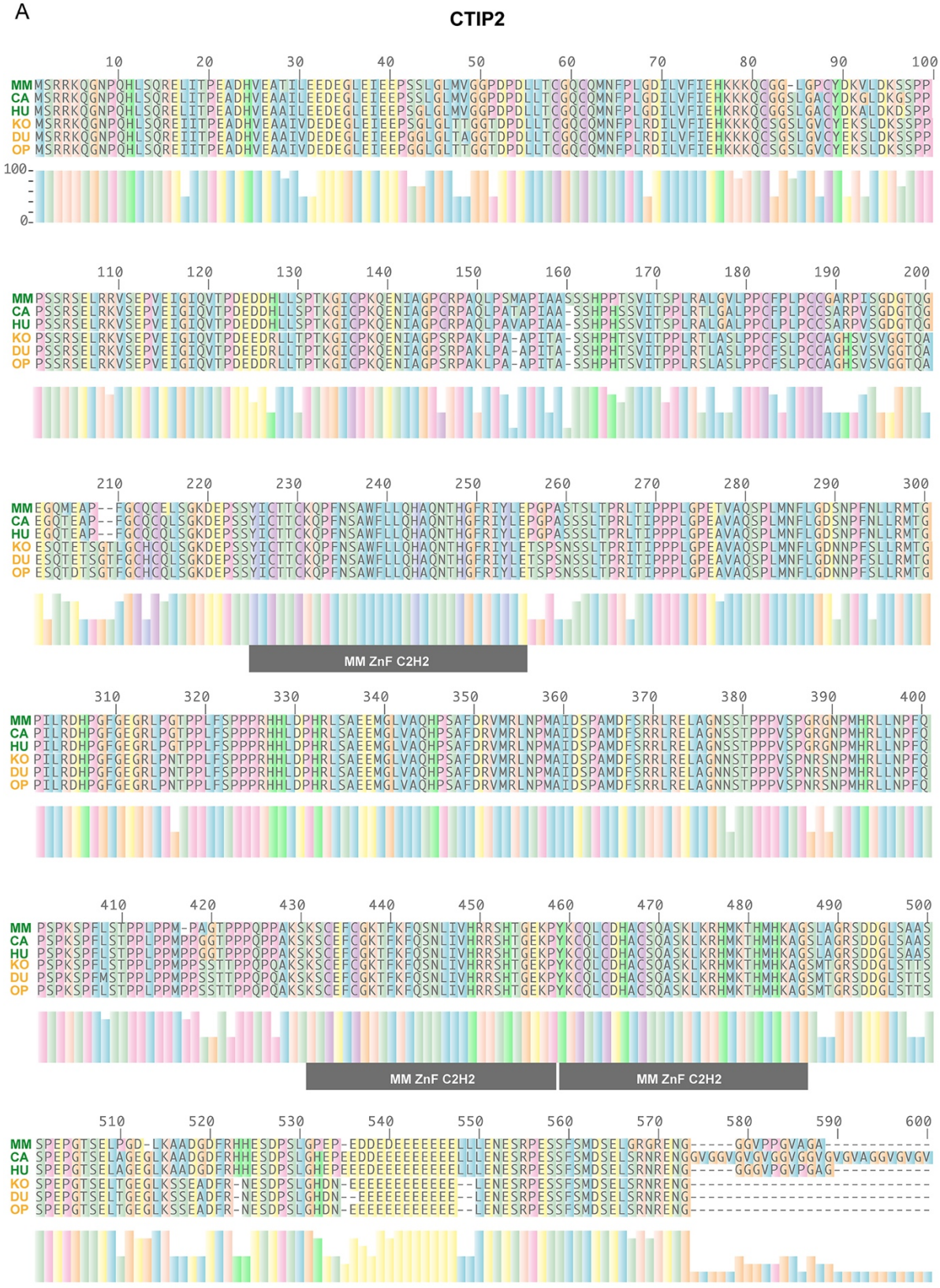

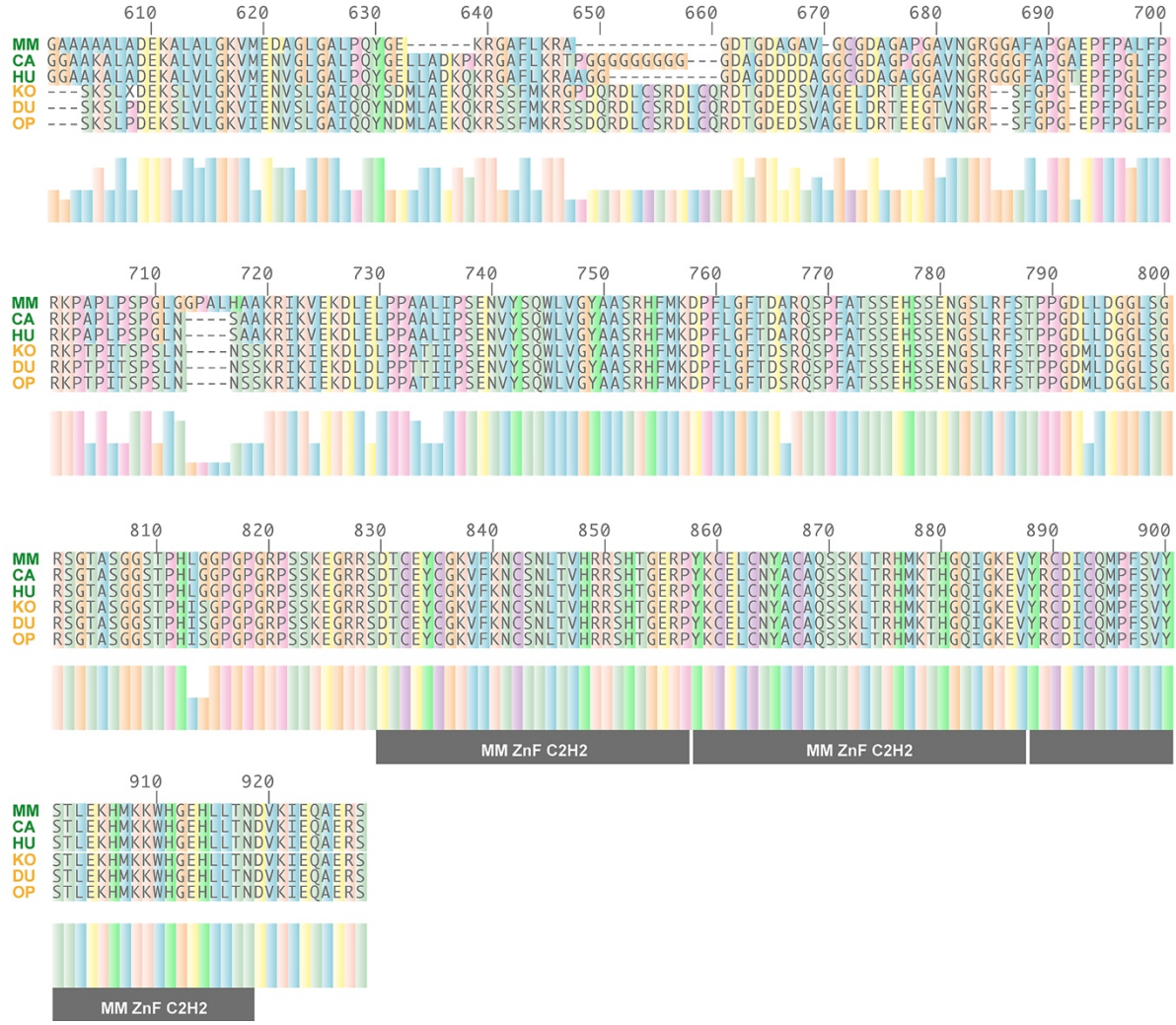
610 620 630 640 650 660 670 680 690 700
MM GAAAAALADEKALALGKVMEDAGLGALPQYGE------KRGAFLKRA----------GDTGDAGAV-GCGDAGAPGAVNGRGGAFAPGAEPFPALFP
CA GGAAKALADEKALVLGKVMENVGLGALPQYGELLADKPKRGAFLKRTPGGGGGGGG---GDAGDDDDAGGCGDAGPGGAVNGRGGGFAPGAEPFPGLFP
HU GGAAKALADEKALVLGKVMENVGLGALPQYGELLADKQKRGAFLKRAAGG---------GDAGDDDDAGGCGDAGAGGAVNGRGGGFAPGTEPFPGLFP
KO ---SKSLXDEKSLVLGKVIENVSLGAIQQYSDMLAEKQKRSSFMKRGPDQRDLCSRDLCQRDTGDEDSVAGELDRTEEGAVNGR--SFGPG-EPFPGLFP
DU ---SKSLPDEKSLVLGKVIENVSLGAIQQYNDMLAEKQKRSSFMKRSSDQRDLCSRDLCQRDTGDEDSVAGELDRTEEGTVNGR--SFGPG-EPFPGLFP
OP ---SKSLPDEKSLVLGKVIENVSLGAIQQYNDMLAEKQKRSSFMKRSSDQRDLCSRDLCQRDTGDEDSVAGELDRTEEGTVNGR--SFGPG-EPFPGLFP
710 720 730 740 750 760 770 780 790 800
MM RKPAPLPSPGLGGPALHAAKRIKVEKDLELPPAALIPSENVYSQWLVGYAASRHFMKDPFLGFTDARQSPFATSSEHSSENGSLRFSTPPGDLLDGGLSG
CA RKPAPLPSPGLN----SAAKRIKVEKDLELPPAALIPSENVYSQWLVGYAASRHFMKDPFLGFTDARQSPFATSSEHSSENGSLRFSTPPGDLLDGGLSG
HU RKPAPLPSPGLN----SAAKRIKVEKDLELPPAALIPSENVYSQWLVGYAASRHFMKDPFLGFTDARQSPFATSSEHSSENGSLRFSTPPGDLLDGGLSG
KO RKPTPITSPSLN----NSSKRIKIEKDLDLPPATIIPSENVYSQWLVGYAASRHFMKDPFLGFTDSRQSPFATSSEHSSENGSLRFSTPPGDMLDGGLSG
DU RKPTPITSPSLN----NSSKRIKIEKDLDLPPTTIIPSENVYSQWLVGYAASRHFMKDPFLGFTDSRQSPFATSSEHSSENGSLRFSTPPGDMLDGGLSG
OP RKPTPITSPSLN----NSSKRIKIEKDLDLPPATIIPSENVYSQWLVGYAASRHFMKDPFLGFTDSRQSPFATSSEHSSENGSLRFSTPPGDMLDGGLSG
810 820 830 840 850 860 870 880 890 900
MM RSGTASGGSTPHLGGPGPGRPSSKEGRRSDTCEYCGKVFKNCSNLTVHRRSHTGERPYKCELCNYACAQSSKLTRHMKTHGQIGKEVYRCDICQMPFSVY
CA RSGTASGGSTPHLGGPGPGRPSSKEGRRSDTCEYCGKVFKNCSNLTVHRRSHTGERPYKCELCNYACAQSSKLTRHMKTHGQIGKEVYRCDICQMPFSVY
HU RSGTASGGSTPHLGGPGPGRPSSKEGRRSDTCEYCGKVFKNCSNLTVHRRSHTGERPYKCELCNYACAQSSKLTRHMKTHGQIGKEVYRCDICQMPFSVY
KO RSGTASGGSTPHISGPGPGRPSSKEGRRSDTCEYCGKVFKNCSNLTVHRRSHTGERPYKCELCNYACAQSSKLTRHMKTHGQIGKEVYRCDICQMPFSVY
DU RSGTASGGSTPHISGPGPGRPSSKEGRRSDTCEYCGKVFKNCSNLTVHRRSHTGERPYKCELCNYACAQSSKLTRHMKTHGQIGKEVYRCDICQMPFSVY
OP RSGTASGGSTPHISGPGPGRPSSKEGRRSDTCEYCGKVFKNCSNLTVHRRSHTGERPYKCELCNYACAQSSKLTRHMKTHGQIGKEVYRCDICQMPFSVY
MM ZnF C2H2
MM ZnF C2H2
910 920
MM STLEKHMKKWHGEHLLTNDVKIEQAERS
CA STLEKHMKKWHGEHLLTNDVKIEQAERS
HU STLEKHMKKWHGEHLLTNDVKIEQAERS
KO STLEKHMKKWHGEHLLTNDVKIEQAERS
DU STLEKHMKKWHGEHLLTNDVKIEQAERS
OP STLEKHMKKWHGEHLLTNDVKIEQAERS
MM ZnF C2H2

B

SATB2

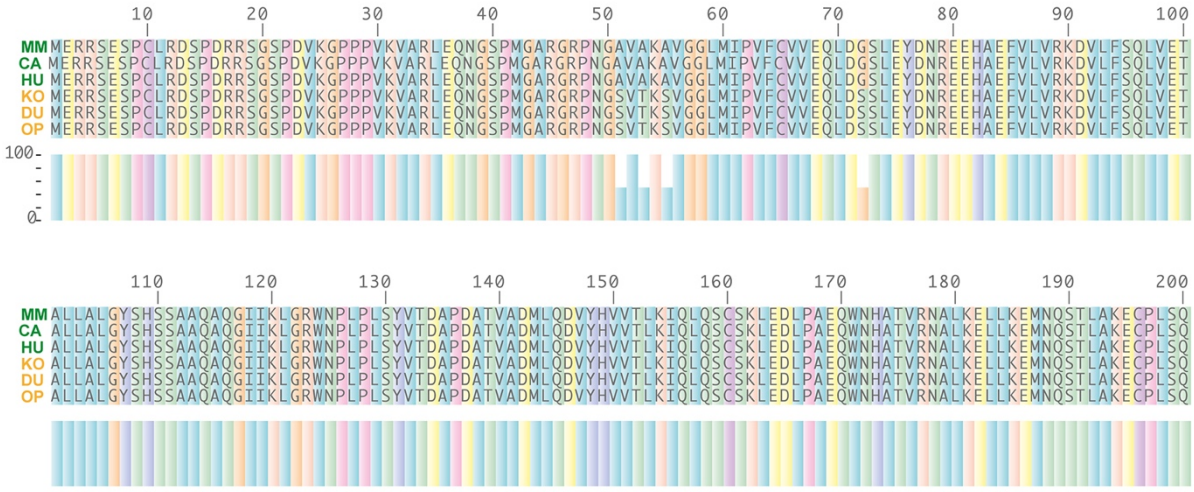
10 20 30 40 50 60 70 80 90 100
MM MERRSESPCLRDSPDRRSGSPDVKGPPPVKVARLEQNGSPMGARGRPNGAVAKAVGGLMIPVFCVVEQLDGSLEYDNREEHAEFVLVRKDVLFSQLVET
CA MERRSESPCLRDSPDRRSGSPDVKGPPPVKVARLEQNGSPMGARGRPNGAVAKAVGGLMIPVFCVVEQLDGSLEYDNREEHAEFVLVRKDVLFSQLVET
HU MERRSESPCLRDSPDRRSGSPDVKGPPPVKVARLEQNGSPMGARGRPNGAVAKAVGGLMIPVFCVVEQLDGSLEYDNREEHAEFVLVRKDVLFSQLVET
KO MERRSESPCLRDSPDRRSGSPDVKGPPPVKVARLEQNGSPMGARGRPNGSVTKSVGGLMIPVFCVVEQLDSSLEYDNREEHAEFVLVRKDVLFSQLVET
DU MERRSESPCLRDSPDRRSGSPDVKGPPPVKVARLEQNGSPMGARGRPNGSVTKSVGGLMIPVFCVVEQLDSSLEYDNREEHAEFVLVRKDVLFSQLVET
OP MERRSESPCLRDSPDRRSGSPDVKGPPPVKVARLEQNGSPMGARGRPNGSVTKSVGGLMIPVFCVVEQLDSSLEYDNREEHAEFVLVRKDVLFSQLVET
100
0
110 120 130 140 150 160 170 180 190 200
MM ALLALGYSHSSAAQAQGIIKLGRWNPLPLSYVTDAPDATVADMLQDVYHVVTLKIQLQSCSKLEDLPAEQWNHATVRNALKELLKEMNQSTLAKECPLSQ
CA ALLALGYSHSSAAQAQGIIKLGRWNPLPLSYVTDAPDATVADMLQDVYHVVTLKIQLQSCSKLEDLPAEQWNHATVRNALKELLKEMNQSTLAKECPLSQ
HU ALLALGYSHSSAAQAQGIIKLGRWNPLPLSYVTDAPDATVADMLQDVYHVVTLKIQLQSCSKLEDLPAEQWNHATVRNALKELLKEMNQSTLAKECPLSQ
KO ALLALGYSHSSAAQAQGIIKLGRWNPLPLSYVTDAPDATVADMLQDVYHVVTLKIQLQSCSKLEDLPAEQWNHATVRNALKELLKEMNQSTLAKECPLSQ
DU ALLALGYSHSSAAQAQGIIKLGRWNPLPLSYVTDAPDATVADMLQDVYHVVTLKIQLQSCSKLEDLPAEQWNHATVRNALKELLKEMNQSTLAKECPLSQ
OP ALLALGYSHSSAAQAQGIIKLGRWNPLPLSYVTDAPDATVADMLQDVYHVVTLKIQLQSCSKLEDLPAEQWNHATVRNALKELLKEMNQSTLAKECPLSQ

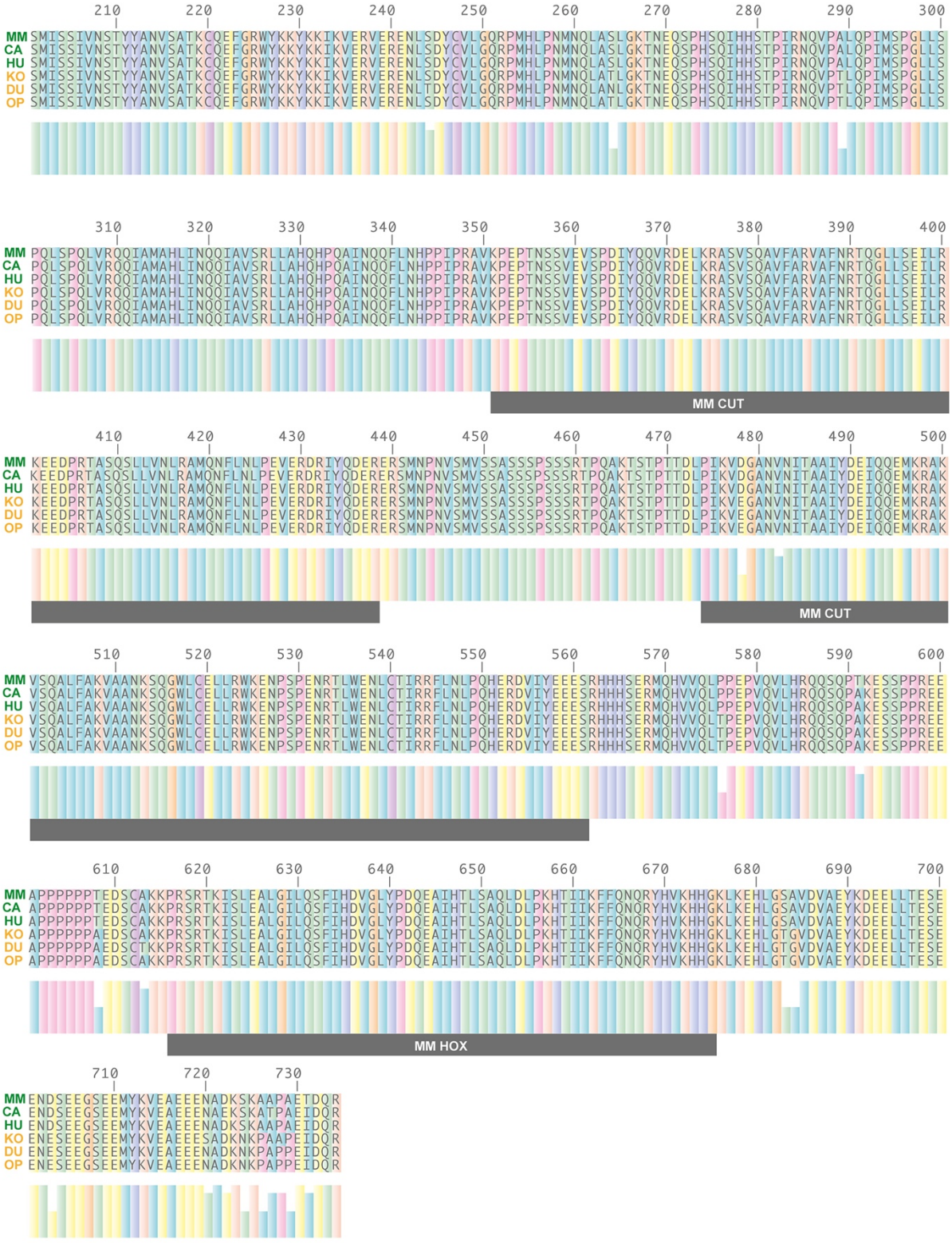

Fig. S1. Full sequence of CTIP2 and SATB2 predicted proteins compared between eutherians and marsupials**.** (*A* and *B*) Full-length predicted proteins of CTIP2 (*A*) and SATB2 (*B*) compared between three eutherians (mouse, MM; dog, CA; human, HU) and three marsupials (koala, KO; fat-tailed dunnart, DU; American opossum, OP). Colors denote different families of amino acids (see methods) and bars underneath reflect the degree of conservation between groups. The functional domains presented in Fig. 1 *C* and *D* are demarcated with black bars.

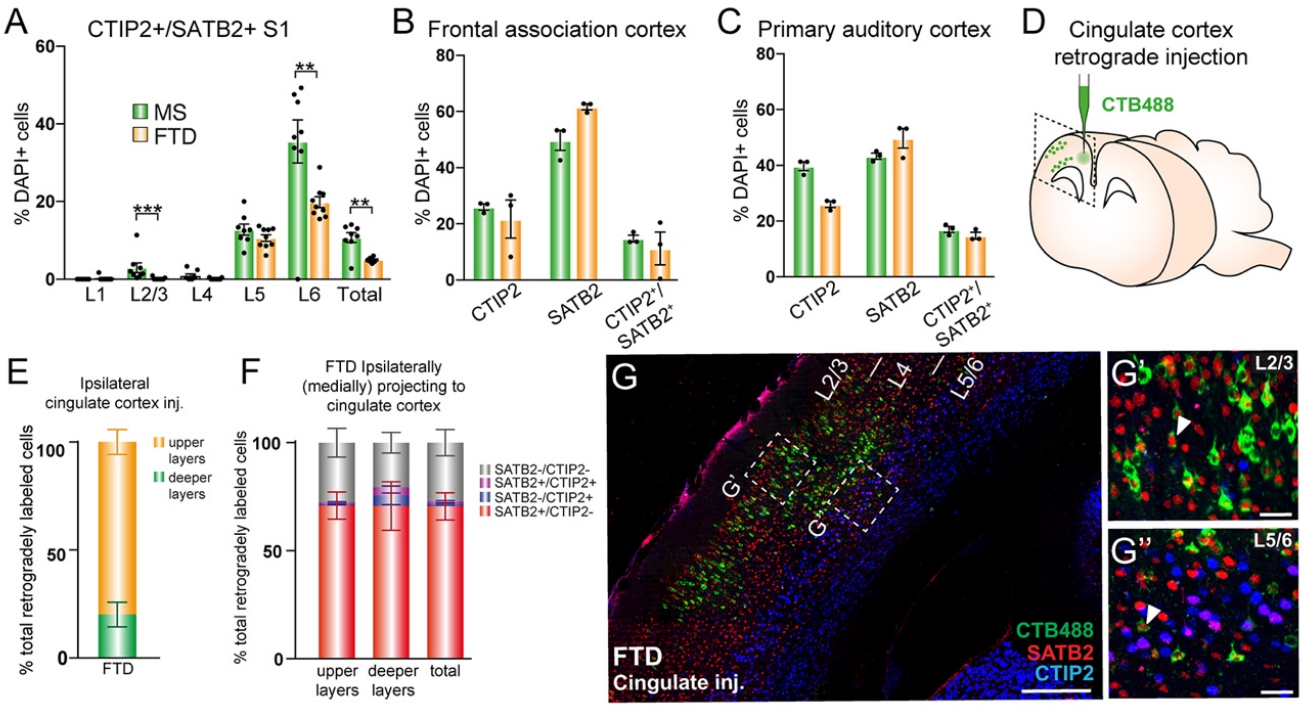

Fig. S2. Characterization of CTIP2 and SATB2 adult expression and ipsilateral medially projecting neurons in the dunnart. (*A*) Number of CTIP2/SATB2 double-positive cells expressed as a percentage of total DAPI-positive cells divided by layers and summed together (total) in the adult mouse (green) and dunnart (yellow) cortex, revealing the similarities and differences between species in the proportion and laminar distribution of coexpressing cells. (*B* and *C*) cell counts of CTIP2 and SATB2 expression in more rostral (*B*) and caudal (*C*) cortical regions revealed similar interspecies trends to the total proportions of expressing cells in S1 (Fig. 2*D*) (*D*) Schematic depicting the experimental protocol, whereby live mature dunnarts were injected with CTB in the cingulate cortex. Cell bodies were then examined more laterally from the site of injection in the same hemisphere (somatosensory cortex) to determine the distribution and expression profile of ipsilateral/medially-projecting neurons. (*E*) Quantification of laminar distribution of retrogradely labeled cells in the somatosensory cortex. (*F*) Quantification of the proportions of the retrogradely labeled population expressing CTIP2, SATB2, both or neither, either in total or divided by upper and deeper layers, reveals a predominance of SATB2 expression in medially projecting dunnart neurons. (*G*) Example images of a dunnart brain injected with CTB in the ipsilateral cingulate cortex, showing retrogradely labeled cells in the upper (*G'*) and lower (*G''*) layers of the cortex, immunostained against SATB2 (red) and CTIP2 (blue). Data are presented as mean ± SEM, n ≥ 3 animals per condition; each scatterdot represents a single animal. Mann-Whitney U tests. ***P* < 0.01; ****P* < 0.001. S1, primary somatosensory cortex; CTB, cholera toxin B; FTD, fat-tailed dunnart; inj., injection; L, layer; Ms mouse. (Scale bars: 250 μm in *G*; 50 μm in *G'* and *G''*).

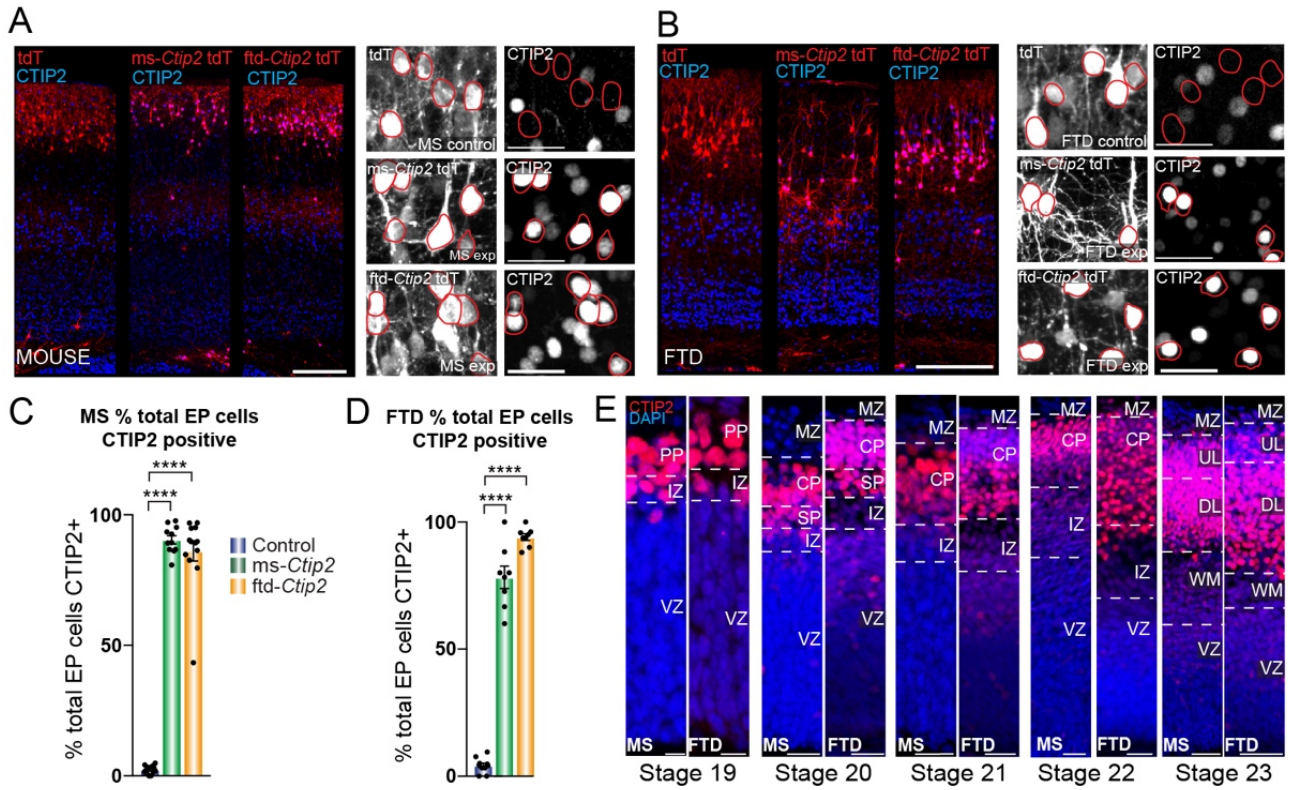

F

	ms-*Ctip2* construct	ftd-*Ctip2* construct	*P* value
ms EP cell CTIP2 intensity	2.952+/-0.1589	3.982+/-0.2587	**0.0015**
ftd EP cell CTIP2 intensity	2.634+/-0.3464	2.859+/-0.2071	0.9551
ms % total EP cells CTIP2+	90.46+/-1.583	86.15+/-3.863	0.5589
ftd % total EP cells CTIP2+	78.25+/-4.389	94.07+/-1.314	**0.0118**
mouse cp axon intensity	1.934+/-0.1671	1.794+/-0.1405	0.5516
mouse ic axon intensity	2.461 +/-0.1710	1.514+/-0.08672	**0.0001**
mouse hn axon intensity	1.442 +/-0.1332	1.788+/-0.07261	**0.031**
ftd cp axon intensity	1.705+/-0.2000	1.646+/-0.2680	0.7308
ftd ic axon intensity	3.402+/-0.6705	10.32+/-1.914	**0.0016**
ftd hn axon intensity	1.319+/-0.08272	1.275+/-0.2490	0.1949

Fig. S3. Cell count of CTIP2-positive cells upon overexpression of *Ctip2* constructs and developmental time course of endogenous CTIP2 expression in the mouse and dunnart**.** (*A* and *B*) Example images of mouse (*A*) and dunnart (*B*) cortex electroporated at stage 23 with TdTomato (tdT) alone or in combination with mouse or dunnart *Ctip2* overexpression constructs and immunostained against CTIP2. (*C* and *D*) Quantification of the percentage of total electroporated cells (tdT positive) positive for CTIP2 protein in control and experimental conditions for mouse (*C*) and dunnart (*D*), revealing the increased number of CTIP2-positive cells upon expression of either construct in both species. (*E*) Cortical sections across five comparable developmental stages (19-23) showing CTIP2 protein expression (red) between mouse and dunnart for each stage, thereby revealing broadly conserved patterns and timing of expression between species. (*F*) Table of means and *P* values following Mann-Whitney U tests comparing the ms-*Ctip2* and ftd-*Ctip2* construct effects on transfected cell intensity of CTIP2, percentage of cells CTIP2+ and axonal fluorescence in ROIs. Data are presented as mean ± SEM, n ≥ 7 animals per condition; each scatterdot represents a single animal. Mann-Whitney U tests. ****$P < 0.0001$. cp, cerebral peduncle; DL, deeper layers; EP, electroporated; exp, experimental; FTD, fat-tailed dunnart; hn, homotopic neocortex; ic, internal capsule; IZ, intermediate zone; Ms, mouse; MZ, marginal zone; PP, preplate; SP, subplate; tdT, tdTomato; UL, upper layers; VZ, ventricular zone; WM, white matter. (Scale bars: *A* and *B,* 250 µm whole cortex (left panels) and 50 µm insets (right panels); *E,* 10 µm for stage 19, 25 µm for stages 20-22, and 50 µm for stage 23).

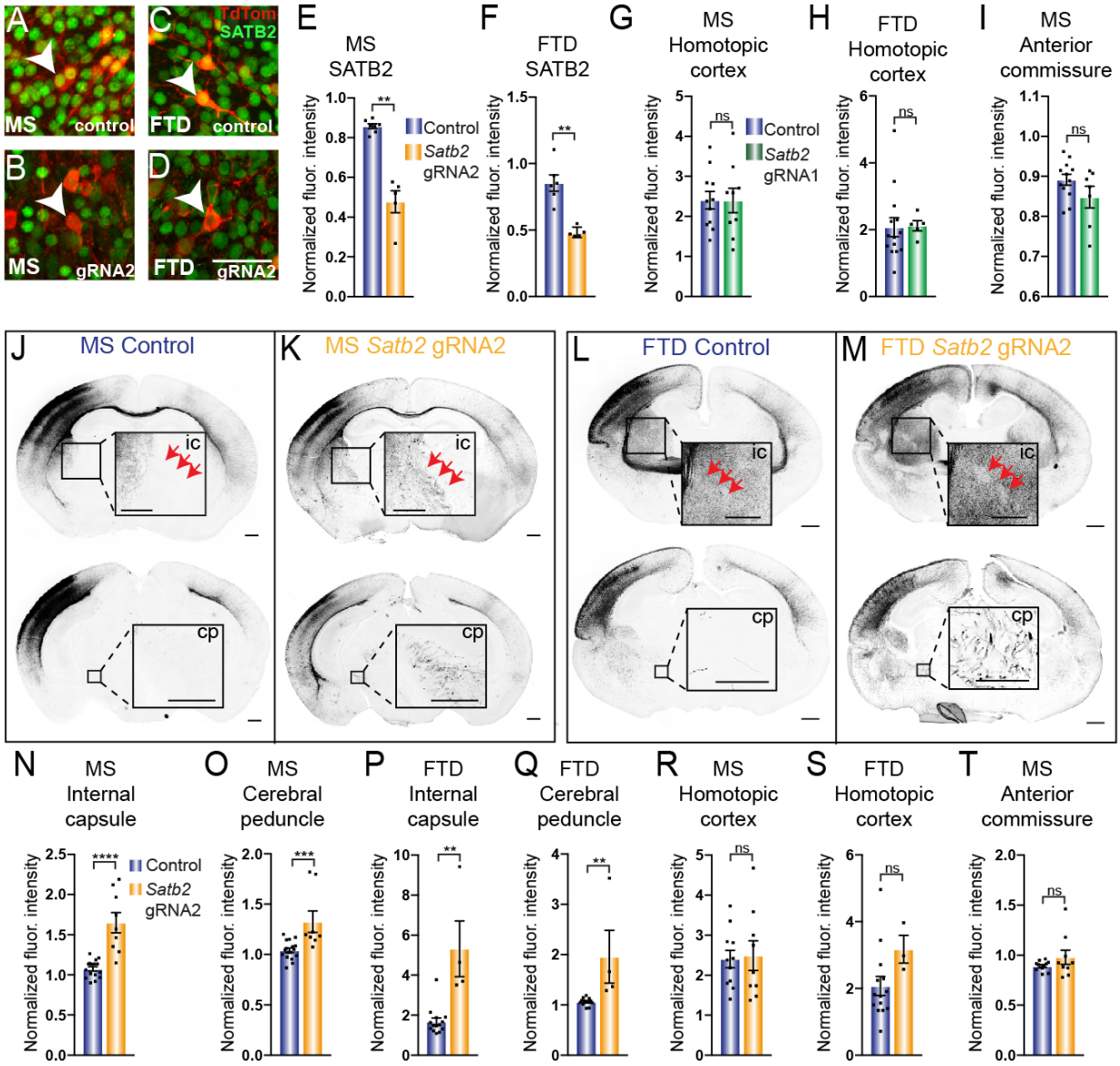

U

	Satb2 gRNA1	*Satb2* gRNA2	*P* value
ms EP cell SATB2 intensity	0.3751+/-0.03079	0.4776+/-0.05543	0.1709
ftd EP cell SATB2 intensity	0.5566+/-0.03312	0.4838+/-0.01734	0.1775
ms cp axon intensity	1.605+/-0.1564	1.326+/-0.1063	0.237
ms ic axon intensity	2.072+/-0.1503	1.651+/-0.1256	0.0653
ms hn axon intensity	2.397+/-0.3045	2.489+/-0.3709	0.9314
ms ac axon intensity	0.8483+/-0.02707	0.9793+/-0.07188	0.1416
ftd cp axon intensity	1.508+/-0.07415	1.959+/-0.5276	0.9273
ftd ic axon intensity	4.064+/-0.6776	5.319+/-1.391	0.5273
ftd hn axon intensity	2.115+/-0.1540	3.172+/-0.4149	0.0714

Fig. S4. Duplication of Fig. 6 experiments with *Satb2* gRNA2 and additional quantification of axon fluorescence intensity for *Satb2* gRNA1 and 2. (*A-D*) Example images of mouse (*A* and *B*) or dunnart (*C* and *D*) brains electroporated at stage 23 with TdTomato (TdTom) alone (control *A* and *C*) or together with a *Satb2* gRNA2 Crispr/Casp9 construct (*B* and *D*), and immunostained against TdTomato and SATB2 (green). (*E-F*) Quantification of intensity of fluorescence of SATB2 immunostaining of control or experimental (gRNA2) electroporated cells, normalized to the intensity of maximally SATB2-expressing non-electroporated cells in mouse (*E*) and dunnart (*F*), revealing a significant decrease in

SATB2 in both species upon overexpression with *Satb2* gRNA2. (*G*-*I*) Quantification of normalized fluorescence intensity of fluorescently labeled axons in the mouse homotopic cortex (*G*) dunnart homotopic cortex (*H*) and mouse anterior commissure (*I*) upon control or gRNA1 electroporation demonstrates no significant change in axon innervation in any of these regions. (*J*-*M*) Example images of control or gRNA2 electroporations in mouse (*J* and *K*) or dunnart (*L* and *M*) at more rostral (upper) or caudal (lower) level. (*N*-*T*) Quantification of axonal fluorescence upon control versus gRNA1 (Fig. 6) electroporation in mouse and dunnart using gRNA2 shows the same effects as found for gRNA1. (*U*) Table of means and *P* values following Mann-Whitney U tests comparing the Satb2 gRNA1 and gRNA2 construct effects on transfected cell intensity of SATB2 and axonal fluorescence in ROIs. Data are presented as mean ± SEM, $n \geq 3$ animals per condition; each scatterdot represents a single animal. Mann-Whitney U tests $^{**}P < 0.01$; $^{***}P < 0.001$; $^{****}P < 0.0001$. ac, anterior commissure; cp, cerebral peduncle; EP, electroporated; FTD, fat-tailed dunnart; gRNA, guide RNA; hn, homotopic neocortex; ic, internal capsule; Ms, mouse. (Scale bars: *A*-*D,* 50 μm; *J*-*M,* 500 μm for whole brains and internal capsule insets; 250 μm for cerebral peduncle insets).

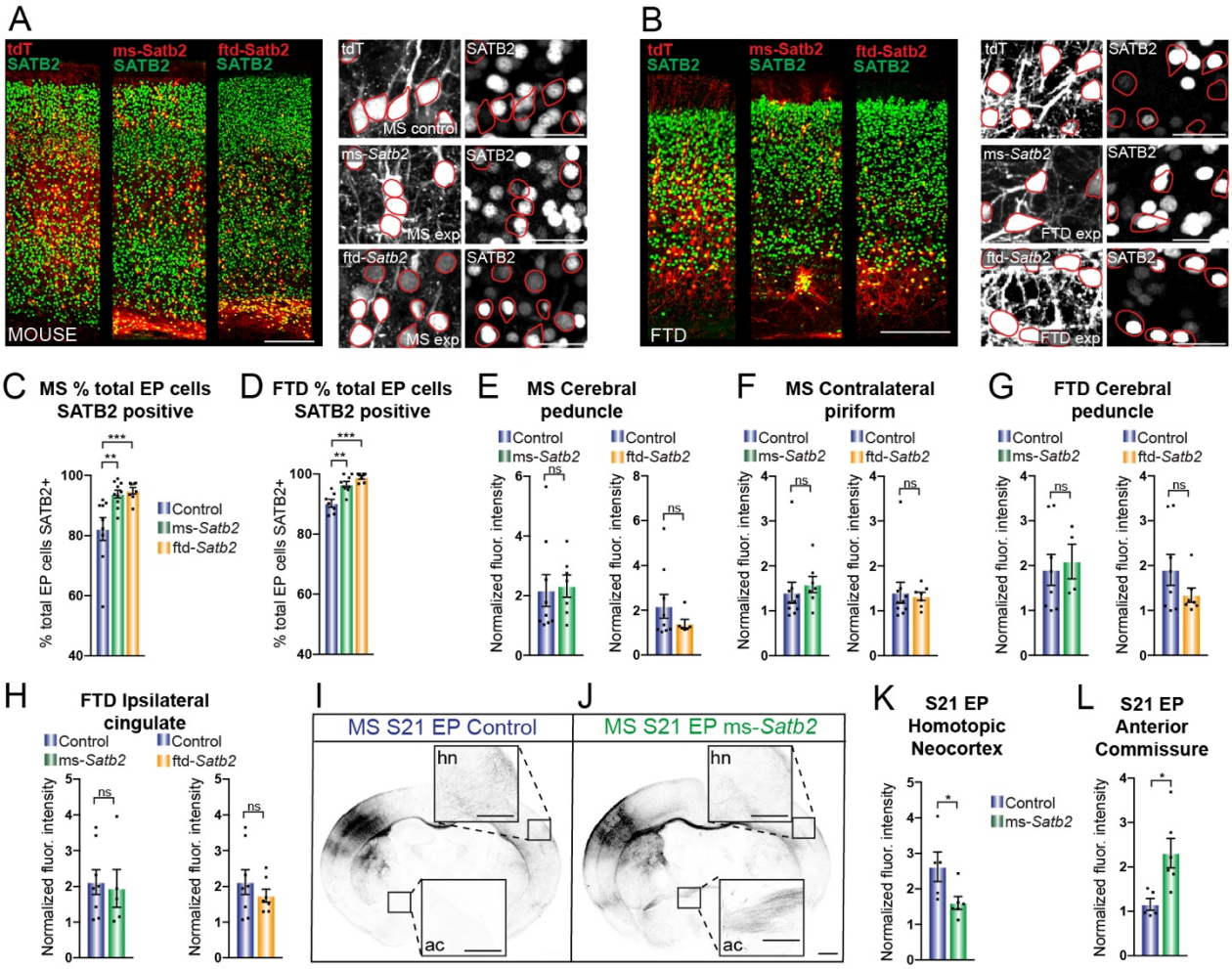

M

	ms-*Satb2* construct	ftd-*Satb2* construct	*P* value
ms EP cell SATB2 intensity	0.6345+/-0.05839	1.043+/-0.09821	**0.0008**
ftd EP cell SATB2 intensity	1.098+/-0.1152	1.704+/-0.08570	**0.0047**
ms EP cell CTIP2 intensity	0.157+/-0.02053	0.1432+/-0.01209	0.9999
ftd EP cell CTIP2 intensity	0.1784+/-0.01838	0.1211+/-0.01983	**0.0426**
ms % total EP cells SATB2+	93.82+/-1.319	94.9+/-1.081	0.8286
ftd % total EP cells SATB2+	96.6+/-0.9157	98.93+/-0.5520	0.0747
ms ac axon intensity	4.04+/-0.6142	4.546+/-1.109	0.8357
ms hn axon intensity	1.737+/-0.2142	1.755+/-0.2581	0.9015
ms piriform axon intensity	1.401+/-0.2338	1.586+/-0.1801	0.2593
ms cp axon intensity	2.323+/-0.3703	1.404+/-0.1924	0.0734
ftd ac axon intensity	4.898+/-1.329	4.795+/-0.5163	0.6389
ftd hn axon intensity	1.563+/-0.1373	1.322+/-0.04180	0.1061
ftd cingulate axon intensity	1.944+/-0.5290	1.739+/-0.1789	0.8763
ftd cp axon intensity	2.092+/-0.3844	1.341+/-0.1589	**0.0424**

Fig. S5. Cell counts and additional areas of axonal fluorescence intensity quantification following stage 20 and 21 *Satb2* overexpression in mouse and dunnart. (*A-B*) Example images of mouse (*A*) and dunnart (*B*) cortex electroporated at S20 (E12) with TdTomato (tdT) alone or in combination with mouse or dunnart *Satb2* overexpression constructs, and immunostained against SATB2. (*C-D*) Quantification of the percentage of total electroporated cells (tdT positive) positive for SATB2 protein in control and experimental conditions for mouse (*C*) and dunnart (*D*) reveals a significant increase in number of SATB2-positive cells upon transfection of either construct in both species. (*E-H*) Quantification of axonal fluorescence intensity in additional brain areas between control and experimental treatments in mouse or dunnart reveals no significant difference in axonal innervation into the mouse cerebral peduncle and contralateral piriform cortex, or the dunnart cerebral peduncle or ipsilateral cingulate cortex following transfection with the *Satb2* overexpression construct of either species at S20 (E12). (*I-J*) Example images of

mouse brains electroporated with control (*I*) or ms-*Satb2* overexpression (*J*) constructs at stage 21 (E13) and collected at stage 28 (P10). (*K*-*L*) Quantification of axonal fluorescence intensity in control and experimental conditions in the homotopic contralateral neocortex (*K*) and anterior commissure (*L*) reveal a significant decrease in axon innervation into the homotopic neocortex and increased ectopic axon projection through the anterior commissure following transfection at stage 21 (E13).
(*M*) Table of means and *P* values following Mann-Whitney U tests comparing the ms-*Satb2* and ftd-*Satb2* construct effects on transfected cell intensity of SATB2 and CTIP2, percentage of cells SATB2+ and axonal fluorescence in ROIs. Data are presented as mean ± SEM, n ≥ 4 animals per condition; each scatterdot represents a single animal. Mann-Whitney U tests. **P* < 0.05; ***P* < 0.01; ****P* < 0.001. Ac, anterior commissure; cp, cerebral peduncle; E embryonic day; EP electroporated; FTD fat-tailed dunnart; hn homotopic neocortex; ic internal capsule; Ms mouse; ns not significant. (Scale bars: *A* and *B* 250 μm whole cortex (left panels) and 50 μm insets (right panels). *I* and *J,* 500 μm for whole brains, 250 μm for homotopic neocortex and anterior commissure insets).

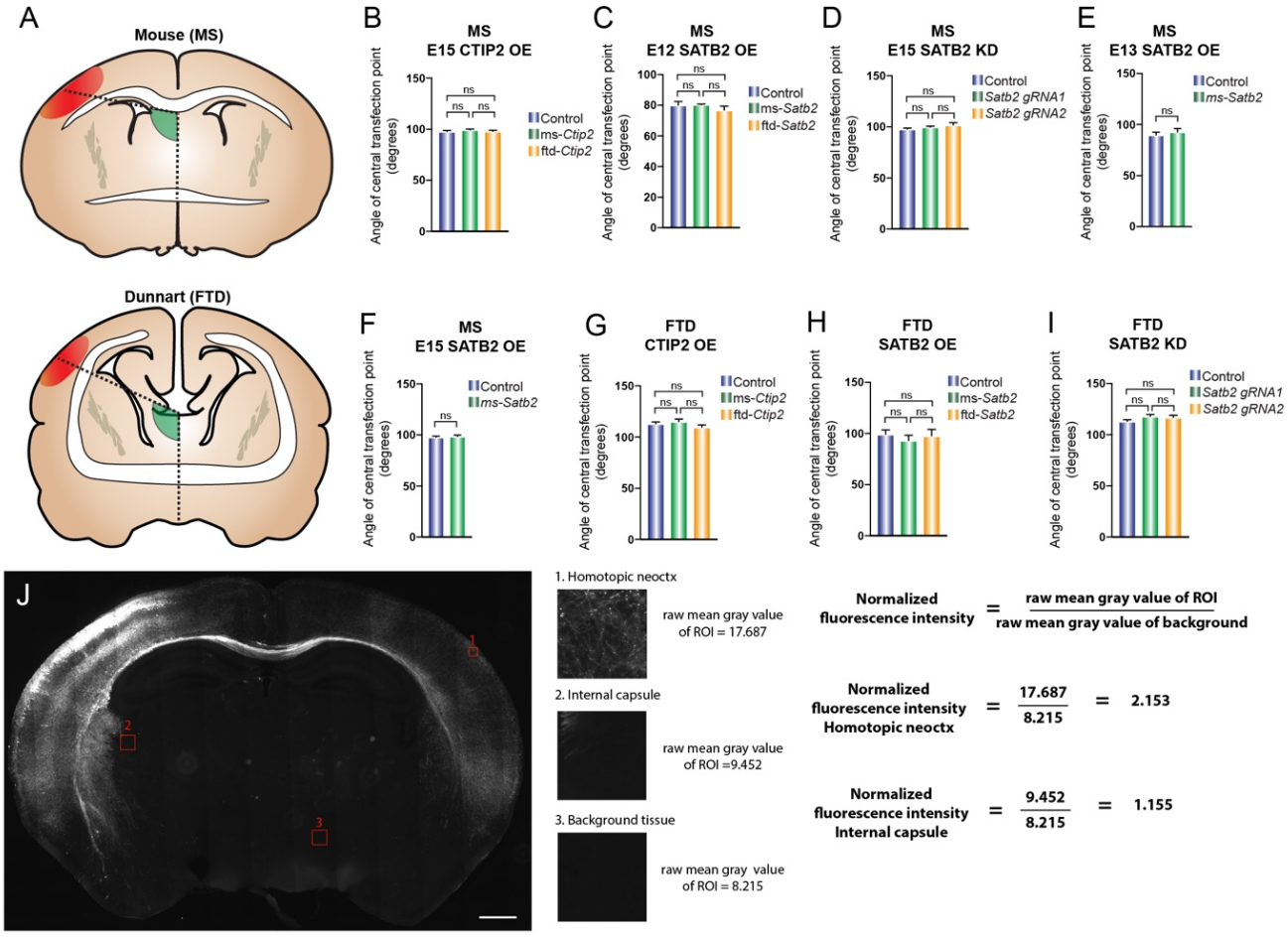

Fig. S6. Quantification of angle of center point of electroporated cell field for all electroporation experiments and schematic of axon fluorescence intensity quantification method. (*A*) Schematic of method of electroporated cell field angle measurement using the base of the corpus callosum/dorsal septum as an anchor point. (*B-F*) The cohort of experimental and control animals in all mouse experiments did not display significant differences in their angles of the transfected field within each experimental group. (*G-I*) The cohort of experimental and control animals in all fat-tailed dunnart experiments did not display significant differences in their angles of the transfected field within each experimental group. (*J*) Example image of a fluorescent microscopy photograph with positioned ROIs to illustrate the quantification method used. After average mean gray values were obtained for each ROI as well as a background region of tissue with no fluorescent axonal labelling, normalized fluorescent intensity values were calculated by dividing the ROI value by the background value. Data are presented as mean ± SEM, n ≥ 4 animals per condition. Mann-Whitney U tests, or t-tests following a D'Agostino-Pearson omnibus normality test, resulted in non-significant differences (ns). KD, knockdown; FTD, fat-tailed dunnart; MS, Mouse; OE, overexpression; ROI, region of interest.

SI Materials and Methods

Animals

Mice

The CD1 wildtype mouse strain was employed for all mouse experiments. This colony is bred at The University of Queensland and time-mated females were obtained by placing male and female mice in the same cage overnight and, in case a vaginal plug was detected, this was considered E0. The day of birth was considered postnatal day (P) 0.

Fat-tailed dunnarts

The breeding and the husbandry of the fat-tailed dunnart (*Sminthopsis crassicaudata;* Dasyuridae), have been described in an article published by our laboratory(1). A breeding colony was established at the Native Wildlife Teaching and Research Facility, The University of Queensland, from founder animals sourced from captive colonies at The University of Newcastle (NSW), Remabi Park (SA), and The University of South Australia (SA), between June 2012 and December 2013. This colony produces between 4-12 new litters per month, each with up to 11 pouch-young. The genetic integrity of the colony is kept via rotation of breeders using the Poiley outbreeding system(2). Breeding boxes were set in a male:female ratio of 1:1 (virgin males) to 1:3 (experienced males) per cage, with cage dimensions of 520 x 335 x 95 (mm). Female dunnarts reach sexual maturity at approximately 5 months (average age of females' first-litter is 210 days), and the first females to conceive per litter were kept as new breeders to select for fertility. Weaned and adult dunnarts not included in mating groups were housed individually in cages containing 10 mm corn cob substrate, shredded newspaper, nest boxes (cardboard tubes and boxes), a sand bowl, a water bowl, a 7-12 cm rock, a food bowl, and a drinking bottle. Animals were fed a daily diet consisting of cat biscuits ad libitum, beef mince-mix (w/w, 78% lean beef mince, 5% ground cat kibble,14% Wombaroo small carnivore food, and 3% of balanced calcium powder; 0.5g for weaners/non-breeders, and 4g lactating females), and live mealworms (*Tenebrio molitor* larvae; 3 for weaners/non-breeders, and 6-10 for lactating females). Additionally, once per week, animals received 5-10 g sunflower seeds, 5-10 g hard-boiled egg and 5-10 g apple. The room was maintained on a 16:8h light:dark cycle, humidity between 30 and 60% and temperature between 22 and 26°C. To optimize breeding success, false winters were set, usually around June and/or December, by gradually reversing the light cycle and dropping temperature by 2- 3°C for 2- 4 weeks. To check for the presence of joeys, females in breeding cages were gently retrieved from a bottomless hiding box with one hand, allowing gentle inspection of the pouch with the

other hand. In non-parous females, the pouch is usually tight and full of pale and dry hair. On the other hand, the pouch of pregnant and oestrous females is easier to open and hairless(3). Females with pouch-young can be detected by a moist pouch and presence of joeys attached to the teats. Teats not used by joeys are small and opaque, while the ones with attached young are prominent and highly vascularised. As soon as joeys were detected in the female pouch, the mothers with pouch young were sent via courier from the Native Wildlife Teaching and Research Facility (UQ, Gatton Campus until December 2017, Hidden Vale Wildlife Centre from January 2018) to the Queensland Brain Institute (UQ, St Lucia Campus).

From developmental stage 18, which corresponds to P0 (day of birth), until the end of stage 27 (P40), dunnart joeys usually remain attached to the same teat, which simplifies the identification of littermates that might have received different treatments. For joeys to be collected after stage 27, when swapping between teats is more common, a tattooing system was used for their identification. One of the paws and/or the base of the tail of each joey was immobilised with forceps and a small scratch was made on the skin with a fine hypodermic needle (30G) embedded with a green tattoo paste.

Animal anesthesia, euthanasia and collection

Deep anesthesia of mice for recoverable procedures, such as *in utero* electroporation, was obtained with an intraperitoneal injection of ketamine/xylazine (120 mg/kg ketamine. and 10 mg/kg xylazine). For sedation of adult female dunnarts with joeys, they were transferred into a gas anesthesia induction chamber with isoflurane 5%, delivered in oxygen at a flow rate of 200 mL/Kg/min. The anesthesia was then maintained by supplying 2-5% isoflurane through a silicone mask throughout the procedure. The system connects directly to the vacuum outlet and incorporates an air brake to avoid the risk of lung collapse. This allows careful examination and manipulation of joeys localised in the pouch in a minimally invasive manner. For terminal collection, the joeys were removed from the teat by gently pulling with forceps and anesthetized with an intraperitoneal injection of sodium pentobarbitone (190 mg/kg), or 5-10 min ice anesthesia for joeys younger than stage 28 (less than P40). Adult dunnarts and mice, as well as mouse pups, were anesthetized with intraperitoneal injection of sodium pentobarbitone. Following deep anesthesia, joeys and mouse pups younger than stage 21 (P15 and E13, respectively) were decapitated and drop fixed in 4% paraformaldehyde (PFA) in 1X phosphate-buffered saline (PBS), while older joeys and mouse pups, as well as adults were anesthetized as above and

transcardially perfused with 0.9% saline (NaCl), followed by 4% PFA. The brains were post-fixed in 4% PFA for four days before being processed.

EdU injections

Time-mated CD1 pregnant dams were injected with EdU (5 µg per 1 g of body weight, diluted in water) at different stages of embryonic development (from stage 18, E10; until stage 26, E18). The dams were restrained and the solution was injected using a 1 mL 27G syringe. The dams were then repositioned in their cages until giving birth to live pups (at approximately E19/P0). Dunnart joeys were exposed carefully and singularly injected intraperitoneally at different postnatal stages (from stage 18, P0-P3; until stage 26, P31-35) with EdU (1 µg per 1 g of body weight, diluted in water). The solution containing EdU was injected using a pulled glass pipette attached to a picospritzer. The mouse pups and the dunnart joeys were then euthanized via transcardial perfusion during stage 27 (P4-P5 for mice, P36-P40 for dunnarts).

Stereotaxic surgeries

Adult mice and dunnarts were anesthetized with isoflurane as described above. They were positioned in a stereotaxic apparatus and their head was immobilized with ear-bars. After having removed the fur on the head, a scalp incision was made in the skin, the skin and the muscles were moved aside and a hole was drilled in the skull above the region of interest. Different brain regions were targeted during stereotaxic injections with a pulled glass pipette attached to a picospritzer and guided by the stereotaxic apparatus. The brain atlas of the stripe-faced dunnart (*Sminthopsis macroura*) was used as an indicative reference for injections in fat-tailed dunnarts(4). The targeted regions were: primary somatosensory cortex (S1), cingulate/motor cortex, and the tectum. The tracers used for the experiments were 0.5-1 µL of 0.5-1.0% cholera toxin subunit B conjugated to a florescent dye (Alexa Fluor 488). Injected animals were then recovered and euthanized via transcardial perfusion after seven days

***In utero* electroporation**

Deep anesthesia of mice was obtained as described above. Full anesthesia was confirmed by toe pinch test, and the dams were placed on a heat pad, which was set at approximately 25°C. The eyes of the dams were covered with Vaseline, in order to prevent drying. Before performing a laparotomy to expose the embryos from the abdominal cavity, the hair covering the abdomen was gently removed using a hair removal cream, the skin

was sterilized with chlorohexidine, and gauze was positioned on the skin, leaving a small circular window for the laparotomy. Once the embryos were exposed, each one of them was positioned so that the lateral telencephalic ventricles were visible through the uterine wall. Plasmid DNA with the addition of 0.0025% Fast Green dye was then microinjected with a Picospritzer II holding a glass pulled pipette, into either the right or left lateral ventricle, depending on the experimental paradigm. The tip of the glass pipette, previously prepared using a Flaming/Brown micropipette puller (heat 495, pull 100, vel 100), was trimmed obliquely using forceps as previously described (5, 6), before plasmid injection. Individual plasmids used and their respective concentrations are listed in table below. The plasmids were then electroporated into the presumptive right or left primary somatosensory cortex (S1) with 3 mm diameter microelectrodes delivering 5 (100 ms, 1 Hz) approximately 36 V square wave pulses from an ECM 830 electroporator. In general, for intralitter identification, the side of electroporation (left or right) was used to distinguish between control and experimental animals. Once this procedure was completed for each embryo, the uterine horns were replaced inside the abdominal cavity and the incision was sutured closed. Animals were then subcutaneously injected with 1 mL of Ringer's solution and recovered in a humidified chamber at approximately 28°C. For pain relief, an edible buprenorphine gel pack was positioned next to the recovering dam in the cage. The buprenorphine edible gel pack was prepared before the surgery by injecting MediGel with 0.2 mL of edible buprenorphine solution (0.026 mg/mL). Dams were then monitored daily until they gave birth to live pups (at approximately E19/P0). The pups were transcardially perfused between P0 and P10, depending on the experimental paradigm, and the brightness, size and position of fluorescent patches in S1 of pups were checked under a fluorescence microscope. Those pups that did not have appropriate size or position of fluorescent patches were excluded from further analyses.

In pouch electroporation

Once the female dunnart was anesthetized and placed on its back, the pouch was carefully everted, and the joeys were exposed gently, without detaching them from the teat. The joeys were electroporated at either stage 20 (P8-11, deeper layer neurogenesis) or stage 23 (P20-P23, upper layer neurogenesis), depending on the experimental paradigm. The joeys were injected with 0.5-1 µL of plasmid DNA in the lateral ventricle using a pulled glass pipette and air pulses delivered via a picospritzer. Similar to *in utero* electroporation, the tip of the glass pipette, previously prepared using a Flaming/Brown micropipette puller (heat 495, pull 100, vel 100), was trimmed obliquely using forceps as

previously described. To visualize the location of the plasmid solution into the lateral ventricle, 0.0025% Fast Green dye was added to 1X PBS. The 1 mm forceps-type electrodes were positioned on the head of each joey immediately following plasmid injection. Unlike *in utero* electroporation in mice, the marsupial joeys can be directly held with the electrodes, without the barriers of the uterine wall and the amniotic sac, such that it is possible to be more accurate while targeting the area of interest by using smaller electrodes. Five 100 ms square pulses of 30-35 V were delivered to specific brain regions via an electroporator system. After the completion of the procedure, the joeys were replaced inside the pouch and the mother was recovered.

Plasmids

PLASMIDS FOR ELECTROPORATION	CONCENTRATION (μg/μL)	SOURCE
pCAG_tdTomato	1	Clontech tdTomato fluorophore subcloned into pCAG by Richards laboratory
pCAG-IRES-GFP-*Satb2* (ftd cDNA)	1	Cloned by Dr Peter Kozulin (Richards lab)
PB-CAG-IRES-GFP-*Ctip2* (ftd cDNA)	1	Cloned by Dr Peter Kozulin (Richards lab)
PB-CAG-IRES-GFP-*Ski* (ftd cDNA)	1	Cloned by Dr Peter Kozulin (Richards lab)
pCAG-*Satb2* (mouse cDNA)	1	Gift from Prof Victor Tarabykin
pCAG-*Ctip2* (mouse cDNA)	1	Gift from Prof Nenad Sestan
pCAG-*Ski* (mouse cDNA)	1	Gift from Dr Suzana Atanasoski

RNA-seq of postnatal dunnart cortex

The cortices of P12 (n = 3) and P20 dunnart (n = 3) were micro-dissected, and individually processed for total RNA extraction using TRIzol reagent (Thermofisher, Waltham, MA) and a RNeasy Minelute kit (74204, Qiagen). The RNA samples were ribo-depleted using Ribo-Zero (15065382, Illumina), fragmented, then cDNA libraries prepared using a Truseq Stranded Total RNA kit v4 (15031048, Illumina), using the low sample (LS) protocol. Sequencing was performed on an Illumina HiSeq 2000 with 125 bp paired-end reads. Cutadapt (version 1.8.1) was used to trim low-quality ends from both ends of the reads (cutoff of 20) and to apply a minimum-length threshold of 36 nucleotides. The transcriptome was assembled *de novo* using the Trinity Software package (version 2.3.2)(7, 8).

Plasmid generation

For the generation of the dunnart-specific *Satb2* overexpression construct, total RNA was obtained from the cortex of dunnart joeys at P25 using TRIzol extraction, and purification with Qiagen Minielute clean-up kit (#74204) followed by DNase treatment (#79254). cDNA was then generated using Superscript III first-strand reverse transcription kit (Invitrogen, #18080-051). Blunt-end PCR products were amplified from P25 dunnart cDNA template using Phusion high-fidelity DNA polymerase (NEB, #M0530), using primers listed in the table below. A single band of ~2.3 kb was visible for *Satb2*. The band was gel-extracted and purified with phenol/chloroform and the PCR product ends were phosphorylated using T4 polynucleotide kinase (NEB, #M0201). The pCAGIG vector was blunt-end digested with EcoRV and the digested plasmid ends were dephosphorylated using Antarctic Phosphatase (NEB, #M0289), for 30 minutes at 37°C. A 1:3, pCAGIG vector : *Satb2* insert blunt-end ligation was setup at 16°C overnight, using a T4 DNA ligation kit (NEB, #M0202). The ligated plasmid was transformed into 20 µl alpha-select competent cells (Bioline, #BIO-85027) and grown overnight at 37°C on LB-agar plates with 100 µg/mL ampicillin. Successful clones were verified with colony PCR and Sanger sequencing.

To generate the dunnart-specific *Ctip2* overexpression construct, total RNA was obtained from the cortex of adult dunnarts. RNA extraction, purification, DNase treatment, and reverse transcription methods were performed as described for *Satb2* above. Nested PCR was used to amplify Ctip2 product from adult cDNA template with Phusion high-fidelity DNA polymerase, using the primers listed in the table below. First, PCR products (~3.1kb) were gel extracted, and used as a template for the nested PCR, using primers containing restriction sites for MfeI and NotI. The nested PCR product was gel extracted (~2.7kb product), the ends of the PCR product digested with MfeI and NotI, and the pPBCAGIG vector digested with EcoRI (isoschizimer for MfeI) and NotI. Both digests were purified using Qiagen PCR clean-up kit. A 1:9, pPBCAGIG vector : Ctip2 insert ligation was setup at 16°C overnight, using a T4 DNA ligation kit (NEB, #M0202). The plasmid transformation and colony verification methods were the same as those described for *Satb2*.

Dunnart-specific SKI was similarly cloned from the total RNA of P25 dunnart cortex. RNA extraction, purification, DNase treatment, and reverse transcription methods were performed as described for the previous transcription factors, using primers listed in the table below. These primers were designed on transcript sequences derived from both the *de novo*-assembled dunnart transcriptome and Sanger-derived sequences of dunnart SKI (see table below). SKI was amplified with a single PCR from the cDNA template using Phusion. PCR products of ~2.3kb were gel extracted and subjected to polyA-tailing (as per

pGEMT protocol, Promega), prior to 1:3 ligation into pGEMT plasmid at 4°C overnight. The ligated plasmid was transformed into alpha-select competent cells, and grown overnight at 37°C on LB-agar plates with 100 µg/mL ampicillin and 80 µg/mL X-gal. Positive colonies were selected and the insert was checked using colony PCR, prior to performing a plasmid miniprep. The SKI insert was digested with AatII, and the DNA ends blunted (NEB, #M1201). The product was column purified and then digested with NotI to fully cut out the insert from pGEMT, followed by gel extraction to isolate the insert. Similarly, pPBCAGIG was digested with XhoI, the DNA ends blunted, then digested with NotI and column purified. A 1:9, pPBCAGIG vector : SKI insert ligation was setup at 16°C overnight, using a T4 DNA ligation kit. The plasmid transformation and colony verification methods were the same as those described for *Satb2*.

PRIMERS FOR GENERATION OF OVEREXPRESSION CONSTRUCTS	
Forward primer ftd-*Satb2* overexpression construct	*TCCGAGTCAAAGTAGCATGG*
Reverse primer ftd-*Satb2* overexpression construct	*CCTGTGCAGCAAAGAAATGTC*
Forward primer ftd-*Ctip2* overexpression construct (1st PCR)	*CCCAACCGGTACAGCTCTC*
Reverse primer ftd-*Ctip2* overexpression construct (1st PCR)	*TGCTTCTCCCCTACAATGCAA*
Forward primer ftd-*Ctip2* overexpression construct (nested PCR)	*GGCCGGCAATTGGATGTCAGTGTAAAT GCC*
Reverse primer ftd-*Ctip2* overexpression construct (nested PCR)	*ATATATATGCGGCCGCGAATGAGGAGG GAAGG*
Reverse primer for ftd-*Ski* Sanger sequencing	*TCGAATCAAAGCTGGGAGGT*
Forward primer ftd-*Ski* overexpression construct	*GAGCCCGATCGCACCATG*
Reverse primer ftd-*Ski* overexpression construct	*GTTCGAGGCACAGGAAGATG*
Forward primer ftd-*Satb2* overexpression construct (colony PCR) *G [Satb2-F]*	*TCCGAGTCAAAGTAGCATGG*
Reverse primer ftd-*Satb2* overexpression construct (colony PCR) *[EGFP-R]*	*GTCCAGCTCGACCAGGATG*
Forward primer ftd-*Ctip2* and ftd-*Ski* overexpression construct (colony PCR) *[pCAG-F]*	*CAACGTGCTGGTTGTTGTG*
Reverse primer ftd-*Ctip2* overexpression construct (colony PCR) *[Ctip2-R]*	*TTTAGCTTCTTTCGGCCTGC*
Reverse primer ftd-*Ski* overexpression construct (colony PCR) *[Ski-R]*	*TCAGTGCAGGAAGGTGTGTG*

Phylogeny and protein conservation analysis

The predicted dunnart protein was translated from the transcript derived from the *de novo*-assembled transcriptome. For SATB2, this was aligned against vertebrate proteins that were either curated (NCBI Reference Sequence NP_631885, NP_001165980 and NP_001122004 for mouse, human and zebrafish, respectively) or predicted only (dog XP_022270795, opossum XP_007494634, Tasmanian devil XP_012400370, koala XP_020849298, platypus XP_028925621). For CTIP2, the translated dunnart protein was similarly aligned against vertebrate proteins that were either curated (mouse NP_001073352, human NP_612808, zebrafish NP_001315335) or predicted only (dog XP_005623848, opossum XP_007473667, Tasmanian devil XP_012405905, koala XP_020862981, platypus XP_028920485). For chicken, the SATB2 sequence was curated (NP_001186039) but the CTIP2 sequence was predicted (XP_003641458).

MUSCLE version 3.8.31 (Edgar 2004) was used to align the predicted dunnart protein sequence against the vertebrate species mentioned above, and MrBayes version 3.2.6 was used to infer phylogeny of these sequences using the parameters: mixed amino acid substitution model, gamma distribution of rate variation, and a Monte Carlo Markov chain analysis run with 1.5 million generations (ngen), sample frequency of 100 and burnin of 4000.

The sequence alignment was repeated using only the predicted dunnart protein sequence against opossum, koala, dog, mouse and human, then analyzed in BIS2Analyzer(9) (http://www.lcqb.upmc.fr/BIS2Analyzer/index.php) in order to visualize the conservation of the protein sequence between eutherians and metatherians. Each amino acid position is color coded according to its physicochemical class (10).

Fluorescence immunohistochemistry and *in situ* hybridization

For dunnart joeys and mouse pups collected after stage 20 (joeys older than P13 and pups older than E12.5), the brains were dissected out of the skull and sectioned in 50 µm coronal slices using a vibratome. Specifically, the brains were embedded in 3.4% agarose and then glued to a magnetic specimen disk and positioned in the vibratome tray filled with 1X PBS. In order to cut the brain coronally, the brains were oriented so that the olfactory bulbs were facing up and the hindbrain was in contact with the surface of the specimen disk. For dunnart joeys and mouse pups collected before stage 20, the brains were left inside the skull and the whole head was embedded into paraffin to be cut in 12 µm slices using a slicing microtome. This procedure reduces the risks of damaging the brains while dissecting them from the skull. Moreover, the slicing microtome allows thinner slices to be

collected (between 10 and 20 μm), thus maximizing the number of sections collected per each brain. A representative section from each brain region, from rostral to caudal, was mounted onto each slide, which were then placed overnight onto a warm plate, to remove excess moisture and ensure that the sections adhered properly to the glass.
For paraffin-embedded sections, the following dewaxing protocol was used before proceeding to fluorescent immunohistochemistry: the sections were embedded in xylene for ten minutes, twice, to allow dewaxing. A gradual rehydration of the sections was obtained by embedding the sections in 100% ethanol for two minutes, twice, followed by 90% ethanol for one minute, 70% ethanol for three minutes and then 1X PBS for five minutes, before post-fixing with 4% PFA for ten minutes. The brain sections that were embedded in 3.4% agarose and cut with a vibratome were mounted on slides and, once dried, incubated in 4% PFA for ten minutes for post-fixation. For both paraffin and agarose-embedded sections, antigen retrieval was performed (when required, depending on the antibody used) in a slide jar containing 0.01M Sodium Citrate, 0.05% Tween 20, pH 6.0, reaching 125°C for four minutes, followed by ten minutes at 90°C. Sections from brains injected with CTB conjugated with Alexa Fluor were antigen-retrieved at lower temperatures to preserve the fluorescent signal of the retrograde tracer: 20 minutes at 80°C, followed by 40 minutes at room temperature. The slides were then incubated for two hours in blocking solution of 10% v/v normal donkey serum (NDS) and 0.2% Triton X-100 (TX100) in PBS (pH 7.4), followed by overnight incubation in 10% normal donkey serum and 0.2% TX100 in PBS with primary antibodies (see table below). After 1X PBS washes (three times for 20 minutes), slides were incubated with appropriate fluorescent secondary antibody; CTIP2 detection sensitivity was improved using a streptavidin-based amplification with donkey anti-rat IgG biotinylated. The secondary antibodies used were: Alexa Fluor 555 donkey anti-rabbit, Alexa Fluor 488 donkey anti-rabbit, Alexa Fluor 568 donkey anti-goat, and Alexa Fluor 647 streptavidin (all 1:500). After 1X PBS washes, the slides were stained for ten minutes with 0.1% 4',6-Diamidine-2'-phenylindole dihydrochloride (DAPI), then washed and coverslipped with antifade mounting media. 50 μm brain sections from dunnart joeys and mouse pups injected with EdU were processed according to the instructions of the Click-iT EdU imaging kit before being incubated with the blocking solution. The detection of EdU is based on a copper-catalysed covalent reaction between an azide and an alkaline.

For in situ hybridization, digoxygenin-labeled antisense riboprobes were transcribed from cDNA plasmids. Primers for dunnart probes were designed based on the RNAseq dataset

generated in the lab and can be found in the table below, while mouse probe primer designs were obtained from the website of the Allen Brain Atlas. Freshly cut 50 µm coronal brain sections were mounted on to SuperFrost Plus slides in RNAse-free conditions. Once the sections were dried, they were fixed with 4% PFA for ten minutes, followed by three washes of three minutes each with 1X PBS. After fixation, the sections were treated with 10 µg/mL Proteinase K in PBS for ten minutes, followed again by three washes of three minutes each with 1X PBS, refixation with 4% PFA for five minutes and three washes of three minutes each with 1X PBS. After these first steps, the slides were incubated for ten minutes in a solution containing 1.33% triethanolamine, 0.02% hydrochloric acid and 0.35% acetic anhydride in MilliQTM H2O, followed by three washes of three minutes each with 1X PBS. The slides were then incubated in 1 mL of hybridization buffer for two hours at 68^{o}C, for pre-hybridization. The hybridization buffer contained: 50% formamide, 5X pH 4.5 Standard Saline Citrate buffer (SSC), 50 µg/mL Bakers'Yeast tRNA, 5X Denhardt's Solution in MilliQTM H2O. Then, 1 µg/mL of riboprobe was diluted into 1 mL of hybridization buffer and incubated at 80^{o}C for five minutes, in order to denature any secondary structures. After the denaturation step, 1 mL of probe solution was applied onto each slide, which were arranged in a chamber humidified with 50% Formamide/5X SCC, and incubated at 68^{o}C overnight. The next day, stringency washes were performed at 68^{o}C. First, the slides were washed in 1% SDS, 50% formamide in 1X SSC for 30 minutes. The next washes were performed with 2X SSC for 20 minutes and then with 0.2X SSC twice, each for 20 minutes. After the stringency washes, the slides were washed in MABT (0.1M maleic anhydride, 0.15M sodium chloride and 0.1% Tween in MilliQTM H2O) three times, five minutes each, at room temperature. The slides were then incubated for two hours in 2% w/v blocking reagent in MABT. After the blocking step, the anti-DIG-AP was diluted 1:4000 in the same blocking solution, which was re-applied onto each slide (~1 mL) and incubated for two hours at room temperature. Following antibody incubation, the slides were washed with MABT at room temperature three times for five minutes, and then incubated in NTMT solution, which contained 0.1M sodium chloride, 0.1M pH 9.5 Tris hydrochloride, 0.05M magnesium dichloride, 0.1% v/v Tween, 2mM imidazole hydrochloride in MilliQTM H2O, for ten minutes at room temperature. To proceed to the color reaction, 1 mL of BM purple, which was previously centrifuged to avoid any precipitate, was added onto each slide. The slides were monitored for between two and 24 hours in order to stop the color reaction whenever the appropriate staining had developed. The slides were then washed for three times with 1X PBS and then coverslipped with ProLong gold mounting media.

ANTIBODIES AND RETROGRADE TRACERS	SOURCE
Rabbit anti-SATB2 (1:500)	Abcam 69995
Rat anti-CTIP2 (1:500)	Abcam 18465
Goat anti-TdTomato (1:1000)	Sicgen 8181-200
Donkey anti-rat IgG biotinylated	Jackson Immunoresearch Inc.
Alexa Fluor 555 donkey anti-rabbit	Invitrogen, Thermo Fisher Scientific
Alexa Fluor 488 donkey anti-rabbit	Invitrogen, Thermo Fisher Scientific
Alexa Fluor 568 donkey anti-goat	Invitrogen, Thermo Fisher Scientific
Alexa Fluor 647 streptavidin	Invitrogen, Thermo Fisher Scientific
Cholera toxin subunit B conjugated to a fluorescent dye (CTB 488)	Invitrogen
0.1% 4',6-Diamidine-2'-phenylindole dihydrochloride (DAPI)	Invitrogen
Anti-DIG-AP	Roche
PRIMERS FOR IN SITU HIBRIDIZATION	
Forward primer ISH probe ms-*Satb2* (Allen Brain Atlas)	GCACACAGGGATTATTGTCAGA
Reverse primer ISH probe ms-*Satb2* (Allen Brain Atlas)	GTGGTACCTCTGGTTCTGGAAG
Forward primer ISH probe ftd-*Satb2*	TCCGAGTCAAAGTAGCATGG
Reverse primer ISH probe ftd-*Satb2*	TGGTTGATGGCTTGAGGGTG
Forward primer ISH probe ms-*Ctip2* (Allen Brain Atlas)	AGTATGGGGAGAAGCGGG
Reverse primer ISH probe ms-*Ctip2* (Allen Brain Atlas)	CTCCTCTCAGCCTGCTCG
Forward primer ISH probe ftd-*Ctip2*	AATGTCCCGCCGCAAACAG
Reverse primer ISH probe ftd-*Ctip2*	GGTTCAAACGCATGACTCTGTC

Microscopy and Image Analysis

Wide-field fluorescence imaging was performed with a Zeiss upright Axio-Imager Z1 microscope fitted with Axio- Cam HRc and HRm cameras and captured with Axio Vision software using MosaicZ. Images were acquired with Zen software (Carl Zeiss AG, Oberkochen). High resolution images were acquired using: 1) 20x/0.75 NA air objective (Nikon) on a Diskovery spinning disk confocal microscope (Spectral Applied Research) built around a Nikon TiE body and equipped with two sCMOS cameras (Andor Zyla 4.2, 2048 x 2048 pixels) and controlled by Nikon NIS software; 2) spinning-disk confocal system (Marianas; 3I, Inc.), consisting of Axio Observer Z1 (Carl Zeiss) equipped with a CSU-W1 spinning-disk head (Yokogawa Corporation of America), ORCA-Flash4.0 v2 sCMOS camera (Hamamatsu Photonics), 20x 0.8 NA PlanApo objectives. Image acquisition was performed using SlideBook 6.0 (3I, Inc). Images were cropped, sized, and

enhanced for contrast/brightness with Photoshop, and the figures assembled in Illustrator (Adobe Creative Suite 6, CA).

All electroporations were aimed at the centre of the somatosensory cortex in both species. The location of this cortical area was determined by adult atlases of the mouse brain, and the closely-related striped-faced dunnart (4), as well as from tracer injection and electrophysiological and architectonic studies showing close conservation of the broad spatial orientation of cortical areas between marsupials and rodents (11, 12) and our own extensive histological examinations of the fat-tailed dunnart (1, 13). Only electroporations with transfected cell fields that were consistently centred on the primary somatosensory cortex were used for subsequent analyses. All animals of both species that had electroporated cell bodies present in the piriform cortex (i.e. below the level of the rhinal fissure) or more anterior olfactory regions (i.e. those that could contribute to the anterior commissure) were excluded from analyses of axon fluorescence intensity.

The electroporated cell fields were evaluated for equivalence of position along the mediolateral extent of the cortex within experimental groups via measuring the angle between the centre of the transfected field and the midline axis of the brain, using either the base of the corpus callosum (mouse) or the base of the interhemispheric fissure (fat-tailed dunnart) as central anchor points and measuring the angle (angle measured colored green in Fig. S6 *A* and *G*). We did not find any significant difference in the angles of electroporated cell fields within any experimental condition (Fig. S6).

Cell counting analyses in specific regions of interest were performed using an unbiased automatic built-in spot detection algorithm in the software Imaris, or manually with a Fiji (Image J) plugin for manual cell count, depending on the experimental paradigm.
The fluorescence intensity of CTIP2 or SATB2 immunostaining in cell electroporated with tdTomato alone or with manipulatory constructs (*Ctip2* or *Satb2* overexpression constructs, mouse or dunnart specific, as well as *Satb2* gRNA1 or gRNA2 Crispr/Cas9 constructs) was measured in the nuclei of both species using Fiji, and then normalized to the maximum value of non-electroporated CTIP2 or SATB2 positive cells for every electroporated construct in both mouse and fat-tailed dunnart.

The fluorescence intensity of axons of cells electroporated with tdTomato alone or with manipulatory constructs was measured at the homotopic contralateral neocortex (ROI =

100 x 100 µm), the internal capsule (174.15 x 174.15 µm), the cerebral peduncle (301.86 x 301.86 µm), the anterior commissure (332.82 x 332.83 µm), cingulate cortex (878.49 x 259.29 µm) and piriform cortex (100 x 100 µm) and normalized to the background intensity value (via division by this value) measured at the level of the basal ganglia (174.15 x 174.15 µm), where no axons were visible. The raw intensity values were obtained by averaging the mean grey value across the entire ROI using the "mean grey value" measurement in Fiji. The formula for obtaining normalized fluorescence intensity values was raw mean grey value of ROI/raw mean gray value of background tissue. The normalized fluorescence intensity of an ROI with an absence of axons would therefore approximate 1 as it would have a similar raw mean gray value as the background tissue. This method of normalization ensured that immunohistochemical/microscopy artefacts that affected the fluorescence intensity of the entire image did not influence the fluorescence intensity of the measured structure, and has previously been used in the quantification of fluorescence intensity of both axons and cell bodies (14, 15). See Fig S6 *J* for a schematic illustrating this quantification method as well as an example calculation for two ROIs.

Statistics

D'Agostino & Pearson tests were used to assess the normality of the datasets. Mann–Whitney or Kruskal–Wallis non-parametric tests were performed in non-normally distributed data, while normal datasets were analysed using Student's t-tests or ANOVAs (Prism 7, GraphPad Software Inc., CA). Probability values of $P < 0.05$ were considered significant. All data is presented as mean ± standard error of the mean (SEM). Further details on the number of replicates per experiment and the tests used for all the analysis are described in the figure legend.

SI References

1. R. Suárez *et al.*, Development of body, head and brain features in the Australian fat-tailed dunnart (Sminthopsis crassicaudata; Marsupialia: Dasyuridae); A postnatal model of forebrain formation. *PLOS ONE* **12**, e0184450 (2017).
2. S. Poiley (1960) A systematic method of breeder rotation for non-inbred laboratory animal colonies. in *Proc Anim Care Panel*, pp 159-166.
3. S. Morton, An Ecological Study of Sminthopsis carasicaudata (Marsupialia : Dasyuridae) III.* Reproduction and Life History. *Wildlife Research* **5**, 183-211 (1978).
4. K. Ashwell, *The Neurobiology of Australian Marsupials: Brain Evolution in the Other Mammalian Radiation* (Cambridge University Press, 2010).
5. H. Tabata, K. Nakajima, Labeling embryonic mouse central nervous system cells by in utero electroporation. *Development, Growth & Differentiation* **50**, 507-511 (2008).

6. A. Matsui, A. C. Yoshida, M. Kubota, M. Ogawa, T. Shimogori, Mouse in utero electroporation: controlled spatiotemporal gene transfection. *J Vis Exp* 10.3791/3024, 3024 (2011).
7. M. G. Grabherr *et al.*, Full-length transcriptome assembly from RNA-Seq data without a reference genome. *Nature Biotechnology* **29**, 644-652 (2011).
8. B. J. Haas *et al.*, De novo transcript sequence reconstruction from RNA-seq using the Trinity platform for reference generation and analysis. *Nature Protocols* **8**, 1494-1512 (2013).
9. F. Oteri, F. Nadalin, R. Champeimont, A. Carbone, BIS2Analyzer: a server for co-evolution analysis of conserved protein families. *Nucleic Acids Research* **45**, W307-W314 (2017).
10. M. Gouy, S. Guindon, O. Gascuel, SeaView Version 4: A Multiplatform Graphical User Interface for Sequence Alignment and Phylogenetic Tree Building. *Molecular Biology and Evolution* **27**, 221-224 (2009).
11. J. Dooley, J. Franca, A. Seelke, D. Cooke, L. Krubitzer, Evolution of mammalian sensorimotor cortex: Thalamic projections to parietal cortical areas in Monodelphis domestica. *Frontiers in neuroanatomy* **8**, 163 (2014).
12. D. M. Kahn, L. Krubitzer, Massive cross-modal cortical plasticity and the emergence of a new cortical area in developmentally blind mammals. *Proceedings of the National Academy of Sciences* **99**, 11429-11434 (2002).
13. R. Suárez *et al.*, A pan-mammalian map of interhemispheric brain connections predates the evolution of the corpus callosum. *Proceedings of the National Academy of Sciences of the United States of America* **115**, 9622-9627 (2018).
14. L. R. Fenlon, R. Suárez, L. J. Richards, The anatomy, organisation and development of contralateral callosal projections of the mouse somatosensory cortex. *Brain and Neuroscience Advances* **1**, 2398212817694888 (2017).
15. J. Nitarska *et al.*, A Functional Switch of NuRD Chromatin Remodeling Complex Subunits Regulates Mouse Cortical Development. *Cell Reports* **17**, 1683-1698 (2016).